Rocking Damage-Free Steel Column Base with Friction Devices: Design, Numerical and Experimental Evaluation

Fabio Freddi[a], Christoforos Dimopoulos[b], Theodore L. Karavasilis[c]
[a] *Department of Civil, Environmental & Geomatic Engineering, University College of London, London WC1E 6BT, UK*
[b] *School of Science, Engineering & Design, Teesside University, Middlesbrough, TS1 3BX, UK*
[c] *Department of Civil Engineering, University of Patras, GR-26500 Patras, Greece*

Keywords: Damage-free column base; rocking; steel frames; seismic design; resilience.

ABSTRACT
Conventional seismic-resistant structures, such as steel moment resisting frames, are designed to experience significant inelastic deformations under strong earthquakes. Inelastic deformations result in damage of structural members and residual interstory drifts, which lead to high repair costs and disruption of the building use or occupation. The aforementioned socio-economic risks highlight the need for widespread implementation of minimal-damage structures, which can reduce both repair costs and downtime. Examples of such structures include steel frames equipped with self-centering beam-column connections, structural fuses, passive energy dissipation devices, self-centering braces, and others. These earthquake-resilient steel frame typologies have been extensively studied during the last decade but little attention has been paid to the behavior of their column bases. Conventional steel column bases are susceptible to experience non-repairable damage significantly affecting the resilience of the entire structure. The present paper presents an innovative rocking damage-free self-centering steel column base and summarize the results of the analytical, numerical and experimental studies. The proposed column base uses post-tensioned high strength steel bars and friction devices respectively to control the rocking behavior and to dissipate the seismic energy. The moment-rotation behaviors of the proposed column base can be easily described by using simple analytical equations allowing the definition of a design procedure for the calibration of the main design parameters with the aim of achieving the damage-free behavior, the self-centering capability and an adequate energy dissipation capacity. A three-dimensional non-linear finite element model of the column base was developed in ABAQUS in order to investigate the local behavior of the components, to validate the moment-rotation analytical equations and to demonstrate the efficiency of the design procedure. On the other hand, a simplified model for the column base was developed in OpenSees and allow to investigate the effects of the proposed column base on a case study building. Nonlinear dynamic analyses show that the rocking column base fully protects the first story columns from yielding and eliminate the 1st story residual story drift without any detrimental effect on peak story drifts. In addition, an experimental campaign under monotonic and cyclic load protocols allows to calibrate the numerical models and further confirms the damage-free behavior and the high potentials of the proposed column base to be used in the design of highly resilient steel structures.

1 INTRODUCTION

The development of innovative minimal-damage seismic resilient structural systems attracted the attention of many researchers in the last decades with the aim of significantly reducing both repair costs and downtime. Examples of such structures include self-centering moment-resisting frames (SC-MRF), systems employing structural fuses, passive energy dissipation devices, self-centering braces, and others (Christopoulos and Filiatrault 2006, Garlock *et al.* 2007, Freddi *et al.* 2013, Chancellor *et al.* 2014, Gioiella *et al.* 2018, Mahdavifar *et al.* 2019). However, despite these earthquake-resilient steel frame typologies have been extensively studied during the last decade, very little attention has been paid to the behavior of their column bases.

Conventional steel column bases typically consists of an exposed steel base plate supported on grout and secured to the concrete foundation using steel anchor rods. The Eurocode 8 allows to design the column bases as full-strength so that plastic hinges are developed in the bottom end of the 1st story columns. This design approach leads to very strong column bases due to the over-strength factors that account for material variability (Latour and Rizzano 2013a) and to severe damage of the column bases significantly

affecting the repairability and hence the resilience of the entire structure. Field observations after strong earthquakes confirmed the susceptibility of column bases to difficult-to-repair damage such as concrete crushing, weld fracture, anchor rod fracture, and base plate yielding (Grauvilardell et al. 2016). Alternatively, Eurocode 8 allows the design of partial-strength column bases, which are designed to develop plastic deformations, however, such design philosophy needs the knowledge of the plastic rotation capacity of the column base under cyclic loading, which is difficult to predict (Kanvinde *et al.* 2012, Latour and Rizzano 2013b, Rodas *et al.* 2016).

In addition to these limitations, previous studies highlighted the importance of the column bases modelling assumptions in the design of steel frames. The stiffness of the column bases is generally difficult to predict and, in conventional designs, they are assumed both rigid or pinned. Under seismic loading, modelling the column bases of a steel moment resisting frame (MRF) as rigid leads to unconservative results in terms of the 1st story drift and collapse resistance (Zareian and Kanvinde 2013). On the other hand, ignoring their rigidity and modelling the column bases as pinned could result in an overconservative design of the columns. Therefore, the current design assumption of perfectly rigid or pinned column bases may produce erroneous results and jeopardize economy, serviceability and safety.

Alternative solutions to the conventional column bases have been presented over the last ten years. Mackinven *et al.* (2007) proposed a steel column base with unbounded steel bars that act as re-centering devices while the column experiences rocking under lateral loads. This column base lacked energy dissipation and developed significant stress concentration during rocking. MacRae *et al.* (2009) proposed a steel column base where a pin was used to resist axial and shear forces. Flexural resistance and energy dissipation were provided by friction due to relative movement of the column flanges with respect to foundation flange plates with slotted holes. This column base had minimal-damage behavior in the strong column axis direction. Yamanishi *et al.* (2012) developed a steel column base that involved exposed yield bolts anchored on a strong plate welded on the column and connected to the foundation anchor bolts through couplers. The yield bolts were the only components experiencing damage and can be easily replaced. In a more recent work, Borzouie *et al.* (2016) presented experimental results on a column base using an asymmetric friction connection. The system experiences rocking and dissipate energy with friction/sliding surfaces parallel to the column strong axis. Superior behavior was achieved under loading in the column strong axis direction, while damage and stiffness degradation were observed under loading in the column weak axis direction. Another class of these innovative column bases utilize post-tensioned (PT) bars to achieve self-centering capabilities, *i.e.*, with negligible residual drifts. For example, Chi and Liu (2012) developed a damage-free steel column base that involves PT bars anchored at the mid-story height and at the bottom of a grade steel beam. Energy dissipation was provided by buckling-restrained steel plates, while shear resistance by bolted keeper plates. Chou and Chen (2011) developed a similar self-centering column base but with PT bars anchored at the top and at the base of the 1st story columns. Lately, Latour *et al.* (2019) experimentally investigates a self-centering base plate connection where friction devices (FDs) were coupled with pre-loaded threaded bars and disk springs in order to provide energy dissipation and self-centering capabilities together with the damage-free behavior. In addition, Kamperidis *et al.* (2019) recently proposed a partial-strength low-damage self-centering steel column base which, in concept, has similarities with the one experimentally tested in this work. Similarly, it employed rocking and PT bars to achieve the self-centering behavior, while the seismic energy was dissipated by hourglass shape steel yielding devices and it uses a different column foot. Wang *et al.* (2019) has presented three different concrete-filled square steel tubular column base connections with PT strands and sandwiched energy dissipaters in the two orthogonal directions. All of the connections demonstrated the typical flag-shape self-centering behavior, with stable energy dissipation while the best performing one showed very low residual drifts (0.15%) even at very large drifts (4%).

A new rocking damage-free steel column base was recently proposed and numerically investigated by Freddi *et al.* (2017a). The proposed system uses PT high-strength steel bars to control the rocking behavior and FDs to dissipate the seismic energy. Simple analytical equations were derived in order to describe the monotonic and cyclic moment-rotation behavior of the column base considering different limit states and allowed to define a step-by-step design procedure. 3D nonlinear finite element (FE) simulations in ABAQUS were performed to validate the analytical moment-rotation equations and to investigate the local behavior of the components. Moreover, a simplified 2D model of the rocking column base was developed in OpenSees in order to perform nonlinear dynamic

analyses on a steel SC-MRF using either conventional or the proposed column base. Dynamic analyses showed that the proposed column base fully protects the 1st story columns and eliminates 1st story residual drifts. In addition, an experimental campaign under monotonic and cyclic load protocols further confirms the damage-free behavior and the high potentials of the proposed column base to be used in the design of highly resilient steel structures. The present paper briefly summarizes some of the research outcomes of the analytical, numerical and experimental work on this innovative damage-free self-centering steel column base.

2 DAMAGE-FREE STEEL COLUMN BASE

Figure 1 shows the column base proposed by Freddi *et al.* (2017a). A thick steel plate with rounded edges is welded on the bottom side of a circular hollow section. The rounded edges avoid stress concentration and damage during rocking.

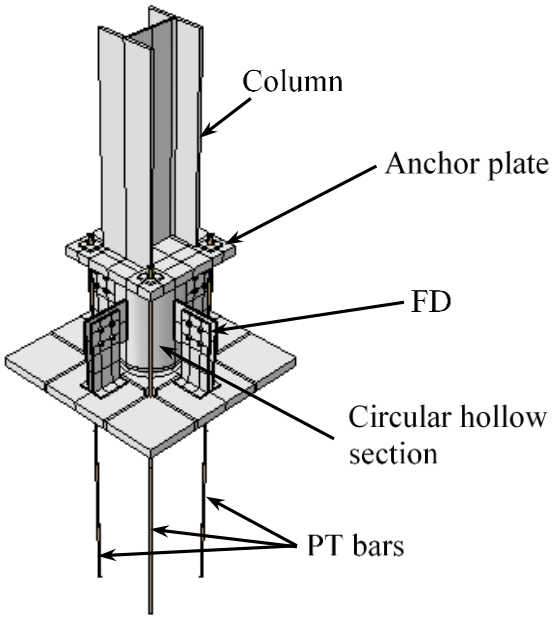

Figure 1. 3D view of the proposed column base

Four PT high strength steel bars are symmetrically placed around the center of the column base to control the rocking behavior. The PT bars are anchored to the bottom of the foundation and to an anchor plate welded on the top of the hollow section. FDs are placed to the four sides of the column base to provide energy dissipation during rocking. The FDs consist of two external steel plates bolted to the base plate; an internal steel plate welded to the circular hollow section; and two plates of brass material in the interface. Rocking of the column base results in sliding of the internal plate with respect to the brass and external plates, and thus, in energy dissipation due to friction. The internal plate is drilled with inclined slotted holes to enable sliding, while the external plates and the brass plates are drilled with aligned rounded holes to accommodate pre-tensioned bolts that are used to tune the friction force. The interested reader can refer to Freddi *et al.* (2017a) for additional details on the geometry of the proposed column base.

2.1 Moment-rotation behavior

Figure 2 shows the dimensions of the column base that control the moment-rotation behavior, *i.e., b* is the dimension of the contact surface; b_{PT} is the distance between the PT bars; b_{FD} is the distance between the centers of the FDs and h_{FD} is the distance of the centers of the FDs from the base plate. Moreover, the forces in the different components when the column base is at the onset of rocking with respect to its right edge are reported. $F_{PT,u}$ and $F_{PT,d}$ are the forces in the PT bars, while $F_{FD,u}$, $F_{FD,d}$ and $F_{FD,c}$ are the forces in the FDs. The subscripts u and d denote whether the point of application of these forces will move upward or downward during rocking. The subscript c denotes the force in central FDs. The lever arms of the forces with respect to the center of rotation $z_{PT,u}$, $z_{PT,d}$, $z_{FD,u}$, $z_{FD,c}$, $z_{FD,d}$ respectively for PT bars and FDs can be derived from simple geometric considerations (Freddi *et al.* 2017a).

The moment-rotation behavior of the column base, up to the design rotation θ_T, is given by the sum by three contributions as reported in Figure 3. The moment is provided respectively by: the axial force, M_N, the PT bars, M_{PT} and the FDs, M_{FD}.

$$M_N = N \cdot b/2 \tag{1}$$

$$M_{PT}(\theta) = 2\left[T_{PT}\left(z_{PT,u} - z_{PT,d}\right) + K_{PT}\left(z_{PT,u}^2 + z_{PT,d}^2\right)\theta\right] \tag{2}$$

$$M_{FD} = 2 \cdot F_{FD}\left(z_{FD,u} + 2 \cdot z_{FD,c} + z_{FD,d}\right) \tag{3}$$

where T_{PT} is the initial post-tensioning force of each PT bar; $K_{PT} = E_{PT}A_{PT}/L_{PT}$ is the stiffness of each PT bar; E_{PT}, A_{PT} and L_{PT} are respectively the Young's modulus, the cross-sectional area and the length of each PT bar while $F_{FD,i}$ is the friction force for each friction surface of the FDs.

The decompression moment, M_E, and the moment at the onset of rocking, M_D, are given by

$$M_E = M_N + M_{PT,0} \qquad M_D = M_E + M_{FD} \tag{4}$$

where $M_{PT,0}$ is the moment provided by the PT bars at zero rotation, *i.e.*, $\theta = 0.0$ in Equation 2. Equations describing the hysteretic moment-rotation behavior of the column base, with and without P-Δ effects, are reported in Freddi *et al.* (2017a).

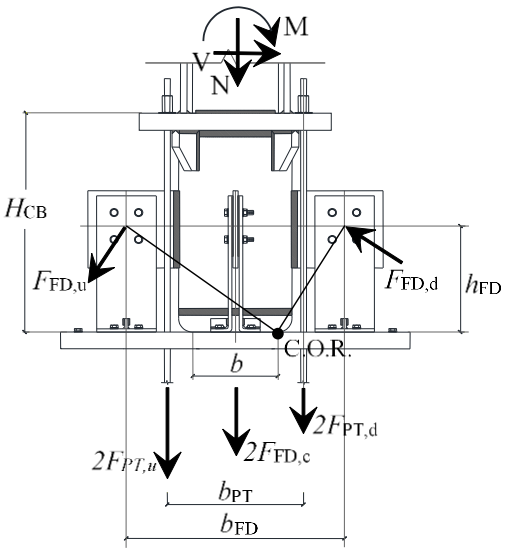

Figure 2. Fundamental dimensions and forces of the column base at the onset of rocking with respect to its right edge

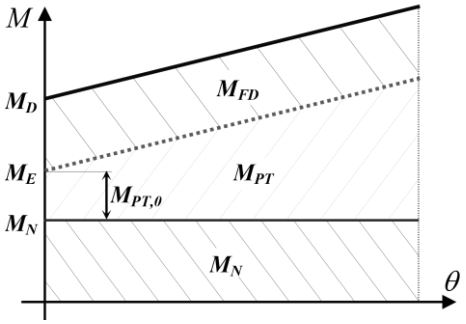

Figure 3. Moment-rotation behaviour of the column base. Moment contribution of the axial force, M_N; of the PT bars, M_{PT}; and of the FDs, M_{FD}

2.2 Design Procedure

The obtained analytical equations allows to define a design procedure for the calibration of the main parameters of the column base with the aim of achieving the damage-free behavior, the self-centering capability and an adequate energy dissipation capacity. The design equations are reported in the following and are based on the non-dimensional parameter $\kappa = \sigma_{PT}/f_{y,PT}$ where σ_{PT} and $f_{y,PT}$ are respectively the stress and the yield stress of the strands.

$$\kappa = \frac{1}{2A_{PT} f_{y,PT}\left(z_{PT,u} - z_{PT,d}\right)}\left[\frac{M_T - 2\frac{E_{PT}A_{PT}}{L_{PT}}\left(z_{PT,u}^2 + z_{PT,d}^2\right)\theta_T}{1+\frac{1}{\alpha_{sc}}} - N_{Ed,G}\frac{b}{2}\right]$$

$$\kappa \le 1 - \frac{E_{PT}\cdot z_{PT,u}\cdot\theta_T}{f_{y,PT}\cdot L_{PT}} = \kappa_{max} \quad \kappa \ge \frac{E_{PT}\cdot z_{PT,d}\cdot\theta_T}{f_{y,PT}\cdot L_{PT}} = \kappa_{min} \qquad (5)$$

where $M_T = M_{N,Rd}/\gamma_T$ is the moment at the target rotation θ_T, $M_{N,Rd}$ is the moment plastic resistance of the column while γ_T is the safety coefficient allows to protect the column from yielding. $\alpha_{sc} = M_E/M_{FD}$ is a design parameter, with a value larger than the unity, that allows to controls the self-centering capability of the column. A_{PT}, L_{PT} and κ are the design variables of the problem *i.e.*, the area of the post-tensioned strands, the length of the post-tensioned strands, and the stress ratio in the strands that allow to define the value of the initial post-tensioning force. While the first equation provide the initial post-tensioning force, the other two equations for κ_{max} and κ_{min} protect the PT bars respectively from yielding and from loss of post-tensioning force for the target rotation θ_T. Additional information about the design procedure is reported in Freddi *et al.* (2017a).

3 EXPERIMENTAL STUDY

3.1 Column base specimen design

A column with cross-section HEB300 was extracted from a prototype building and used to define the specimen of the experimental study. The minimum and maximum axial forces, N_{Ed}, deriving from the seismic load combination were equal to 510.3 kN and 565.3 kN, respectively. The axial force due to the gravity loads of the seismic load combination, $N_{Ed,G}$, was equal to 537.8 kN.

The experimental test was conducted on a 3/5 scaled model of the full-scale prototype column base (*i.e.*, scaling factor $\lambda = 0.6$) and the specimen used in the experimentation was designed according to the dimensions of the scaled column cross-section, the scaled values of the axial forces N_{Ed} and $N_{Ed,G}$, and the target drift defined for the prototype building. The scaling factor $\lambda = 0.6$ was chosen based on the Lab capabilities and the scaling was made in accordance with the constant stresses and acceleration similitude.

The column base chosen for the experimental test was a UC 203×203×46, which has similarities with the dimensions of the prototype column base HEB 300 scaled by λ. The scaled axial forces N_{Ed} and $N_{Ed,G}$ were equal to 203.5 kN and 193.6 kN, respectively. The target rotation was assumed equal to θ_T = 0.03 rad. The bending moment resistance $M_{N,Rd}$ evaluated according to the Eurocode 3 was equal to $M_{N,Rd,y}$ = 176.58 kNm and $M_{N,Rd,z}$ = 81.97 kNm in the strong and weak column axis, respectively.

Based on the geometry of the column cross-section, the fundamental dimensions of the column base (*i.e.*, b, b_{PT}, b_{FD}, and h_{FD}) were selected with respect to practical and geometric considerations. A circular hollow section with 193.7 mm diameter and 30 mm thickness was adopted. A circular steel plate with the same diameter was welded at the bottom of the hollow section. Standard mechanical

processing provides this plate with rounded circular edges having a radius of 30 mm as well as with appropriate space to accommodate the shear key. The contact surface has a dimension b equal to 143 mm. Due to the reduced availability of PT bars of small dimensions, 7 wire strands satisfying the requirements of the BS 5896 (BSI Standards Publication, 2012) were used in the experiment. The anchor plate of the PT strands in the top of the hollow steel section was rectangular and has width, length and thickness equal to 330 mm, 415 mm and 50 mm, respectively. The distance among the strands b_{PT} was selected equal to 255 mm. Table 1 provides the material properties assumed for the design (f_y: yield stress; f_u: ultimate stress; E: Young's modulus) according to test certificates provided by the suppliers.

The design procedure, previously illustrated, was used for the definition of the properties of the column base and Figure 4 shows the variation of κ with respect to L_{PT} for the 7 wire strands of 9.3 mm used in the experiment, (equivalent area of A_{PT} = 52 mm^2). The coefficients γ_T and γ_{sc} were assumed respectively equal to 1.165 and 1.10. The design procedure provides L_{PT} equal to 805 mm and κ equal to 0.2175 (T_{PT} = 21.3 kN).

Figure 5 shows the moment-rotation behavior for the column base. The decompression moment, M_E, the moment at the onset of rocking, M_D, and the moment provided by the FDs, M_{FD}, were equal to 19.94 kNm, 38.07 kNm and 18.13 kNm, respectively.

Table 1. Design properties of the materials

Elements		f_y [MPa]	f_u [MPa]	E [GPa]
Column & plates	S355JR	355	510	210
PT strands	BS5896: 2012	1885	1995	195
Bolts	Class 10.9	900	1000	210
Brass	C46400	200	450	100

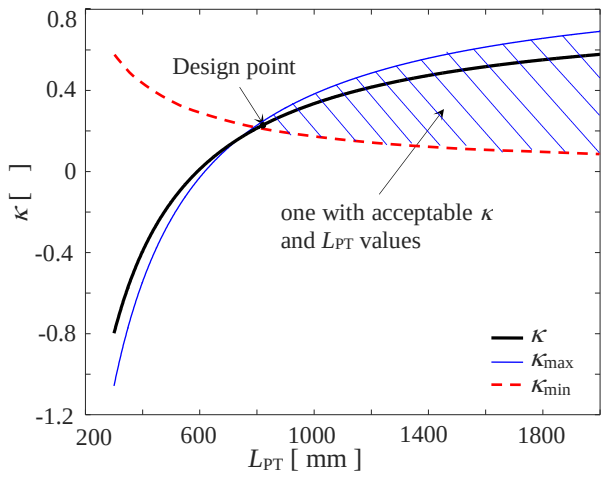

Figure 4. Variation of κ with respect to L_{PT} for A_{PT} = 52 mm^2

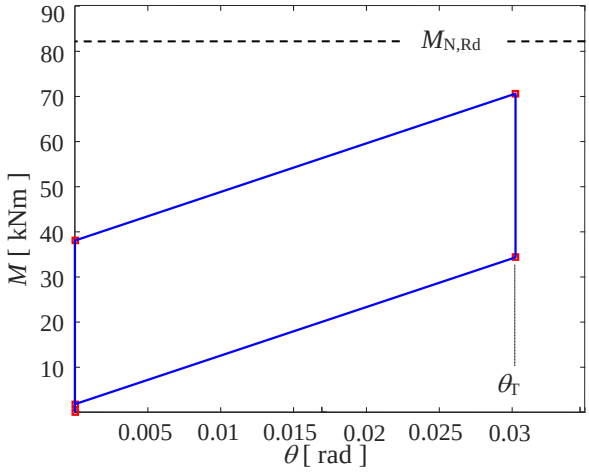

Figure 5. Hysteretic moment-rotation behaviour of the designed column base

M_{FD} was derived by M_E and α_{sc}, then, the FDs were designed by selecting appropriate values of the parameters of Equation 3. FDs were introduced on the four sides of the column base and the relevant dimensions were b_{FD} = 465 mm and h_{FD} = 250 mm. The required friction force in each of the four FDs was F_{FD} = 10.87 kN. The thickness of the internal and external plates of the FDs were 10 mm and 8 mm, respectively. Two 3 mm thick brass plates were used as friction interfaces and two M12 class 10.9 bolts were used to apply the pre-loading force by tightening. The friction coefficient at the brass-steel interface was evaluated by preliminary tests described in the next section. The pre-loading force was defined based on the friction coefficient in order to achieve the required friction force. The dimensions of the slotted holes were designed to allow a large rotation (*i.e.*, close to 0.06 rad) without bearing of the bolts on the plates.

3.2 Friction device characterization tests

In order to define the value of the friction coefficient, μ_{FD}, for the investigated materials and to assess its stability, cyclic tests were performed on an isolated FD. These preliminary tests use a configuration, materials and bolts that were similar to the one employed in the large scale test of the column base.

Quasi-static tests using four values of the pre-loading force in each bolt were performed spanning from 10 to 25 kN; thus, obtaining different values of the clamping force acting on the sliding surface. The axial force in the bolts, N_b, was monitored with load cells during the tests. The friction coefficient was determined as

$$\mu_{FD} = F_{FD} / m \cdot n \cdot N_b \qquad (6)$$

where $m = 2$ is the number of surfaces in contact and $n = 2$ is the number of bolts. Figure 6 shows the normalized force history obtained according to Equation 10 with respect to applied displacement. Consistent results were obtained also for the other pre-loading force values. From this figure it can be concluded that the friction coefficient is equal to 0.25.

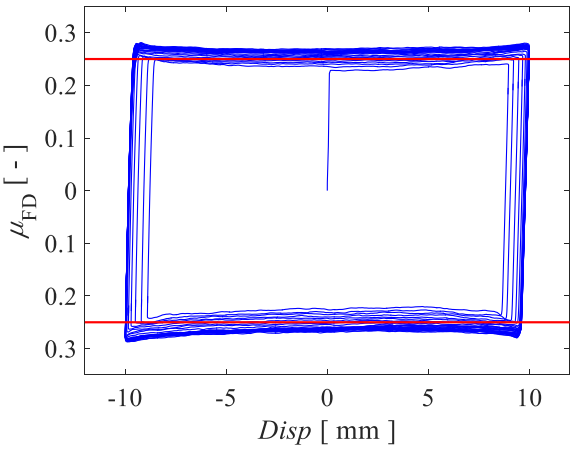

Figure 6. Friction device characterization test. Normalized force history for the definition of the friction coefficient

3.3 *Column base tests*

Experiments on the proposed rocking damage-free steel column base with FDs were conducted in the test setup shown in Figure 7 and in Figure 8.

Two external PT bars with diameter of 15 mm (A_{PT} = 177 mm^2) and yield and ultimate strength equal to f_y = 900 MPa and f_u = 1100 MPa, were introduced to simulate the axial force due to the gravitational load. The PT bars were connected to the upper beam, which transfers the force to the column, and to two anchor supports connected to the strong floor. Hollow hydraulic jacks were used in order to apply the post-tensioning force and the load cells were used to measure and to calibrate the initial force and to control its variation during the tests. The column was placed on a steel basement provided with anchor plates for the strands. The strands were post-tensioned through hollow hydraulic jacks and four load cells were interposed between the anchor grips and the anchor plates in order to calibrate the initial post-tensioning force and to measure the force variation along the tests. The pre-loading force in the FDs was applied through a calibrated torque wrench. Additional four load cells were used to measure the variation of the axial force in the two bolts of two friction devices during the tests.

A horizontal actuator connects the specimen to a reaction wall. Displacement transducers were placed on the base of the column in order to measure horizontal translations and rotations in the longitudinal direction, as well as, horizontal translations in the transverse direction and torsions.

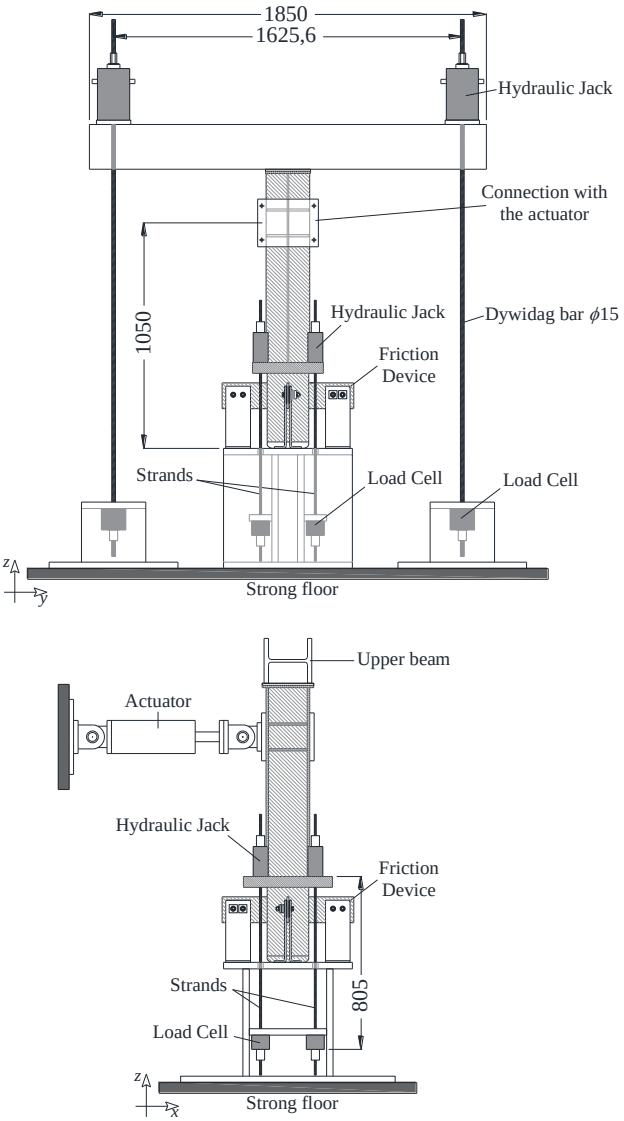

Figure 7. Front and lateral view of the column base's tests setup (dimensions in mm)

Figure 8. Full test setup

Moreover, in order to evaluate the stresses and deformation of the circular hollow cylinder of the column base, four strain gages were introduced in the position close to the pivot points of the rocking at each side.

Quasi static experimental tests were performed on the column base with and without strands and FDs in order to decouple the moment contributions from each component. Preliminary tests were performed with amplitudes ranges within the elastic behavior of the strands. A final test with cyclic displacements of increasing amplitude was conducted showing the damage-free behavior of the column base up to the design rotation. For amplitudes higher than the design rotation, yielding of the strands occur, while, for very large rotation the failure was observed in the FDs due to bolts bearing.

3.4 Comparison with ABAQUS model

A numerical model of the column base was developed in ABAQUS and the modeling procedure is thoroughly described in Freddi *et al.* (2017a). Figure 9 shows the comparison between the experimental and numerical results in ABAQUS. It is worth noticing that, even before the calibration, the ABAQUS model allows a quite accurate prediction of the column base's behavior in terms of maximum moment and dissipation capacity but it lacks in correctly capturing the initial stiffness.

Imperfections can significantly affect the initial stiffness of steel structures and hence, their effect was evaluated according to the EN 1090-2 (2008) and included in the numerical ABAQUS models for the column base. The considered imperfection consists in a geometrical deviation in the plate with rounded edges and affects the contact conditions.

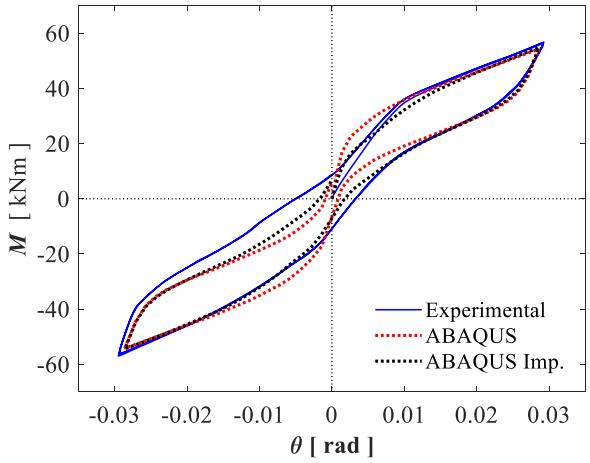

Figure 9. Moment-rotation behavior of the column base up to the design rotation. Comparison of experimental and numerical results

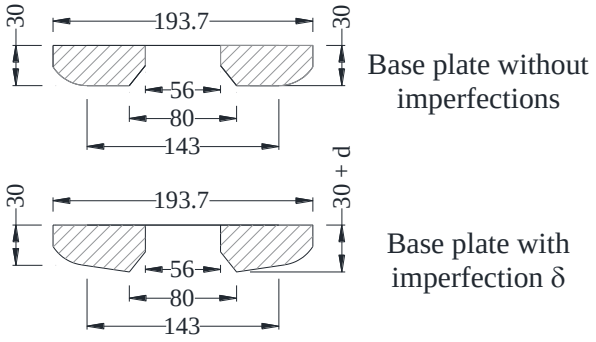

Figure 10. Imperfections modelling. Geometrical deviation in the plate with rounded edges

Without the imperfection, the central part of the steel plate with rounded edges is flat and in full contact with the steel basement, differently, in the model accounting for the imperfections, the contact surface is limited before rocking. The local imperfection was modelled as a symmetrical geometrical deviation as shown in Figure 10. Several geometrical deviation amplitudes δ were investigated, *i.e.*, 0.3 mm, 0.7 mm, 1.0 mm and 1.4 mm and compared with the 'perfect' model (δ = 0.0 mm). Figure 9 shows also the comparison of the experimental results with the numerical results for the 'perfect' model and the model with a geometrical deviation with amplitude δ = 0.3 mm. This comparison shows that the 'perfect' model provides larger initial lateral stiffness, however by accounting for the imperfections is possible to correctly represent the initial stiffness of the system and predict more accurately the hysteretic behavior of the column base.

4 NONLINEAR DYNAMIC ANALYSES

A simplified model for the column base was developed in OpenSees and was used to investigate the effects of the proposed column base on the seismic response of a case study building. A detailed description of the OpenSees model was reported in Freddi *et al.* (2017a).

4.1 Case study building

A 5-story, 5-bay by 3-bay prototype steel building having two identical perimeter seismic-resistant frames in the *x* direction as reported in Figure 11 was selected as case study. The study focuses on one perimeter seismic-resistant frame. This frame was designed as a SC-MRF using PT beam-column connections with the aid of the design procedure proposed by Tzimas *et al.* (2015). The interior gravity frames (with pinned beam–column connections and pinned column

bases) were coupled with the SC-MRF through the floor diaphragm.

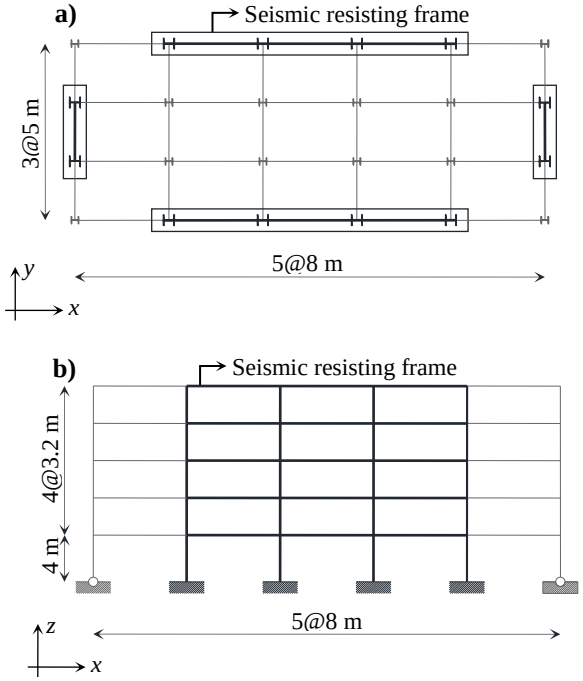

Figure 11. (a) Plan view; and (b) elevation view of the prototype building

4.2 *Models for the SC-MRFs and earthquake ground motions*

FE models for the SC-MRFs were developed in OpenSees (McKenna et al. 2006). The models used fiber beam-column elements for the beams and columns, while appropriate combinations of zero-length nonlinear rotational springs were used for the panel zones, the PT beam-column connections, and the locations where beam plastic hinges were expected. More information on modeling SC-MRFs in OpenSees can be found in (Dimopoulos *et al.* 2013, Dimopoulos *et al.* 2016, Tzimas *et al.* 2015, Freddi *et al.* 2017a). The SC-MRF with conventional column bases has T_1 equal to 0.94 sec, while the SC-MRF with the rocking column bases has T_1 equal to 0.867sec. The latter difference was due to the shorter flexible length of the first story columns of the SC-MRF with the rocking column bases. Ten earthquake ground motions (selected from the far-fault ground motions developed by the FEMA P695 project (FEMA P695 2008)) were used for nonlinear dynamic analyses. These earthquake ground motions were scaled to the Design Based Earthquake (DBE; probability of exceedance of 10% in 50yrs) and Maximum Credible Earthquake (MCE) seismic intensities. The design basis earthquake is expressed by the Type 1 elastic response spectrum of Eurocode 8 with peak ground acceleration equal to 0.35g and ground type B. The maximum credible earthquake (MCE) is assumed to have intensity equal to 150% the DBE intensity. The spectral acceleration $S_a(T_1)$ corresponding to the fundamental structural period and damping ratio equal to 3% is selected as intensity measure (Freddi *et al.* 2017b).

4.3 *Seismic analyses results*

Figure 12 (a) and (b) show respectively the residual story drifts of the SC-MRFs without and with the proposed column bases. It can be observed that the SC-MRF with conventional column bases experiences appreciable residual 1st story drifts due to 1st story column yielding. Such residual drifts reach values close to 0.5% under individual earthquake ground motions (*i.e.*, a critical value that is considered as the limit beyond which repair of a steel building may not be economically viable (Dimopoulos *et al.* 2016). On the other hand, the use of the rocking column base essentially eliminates the 1st story residual drift.

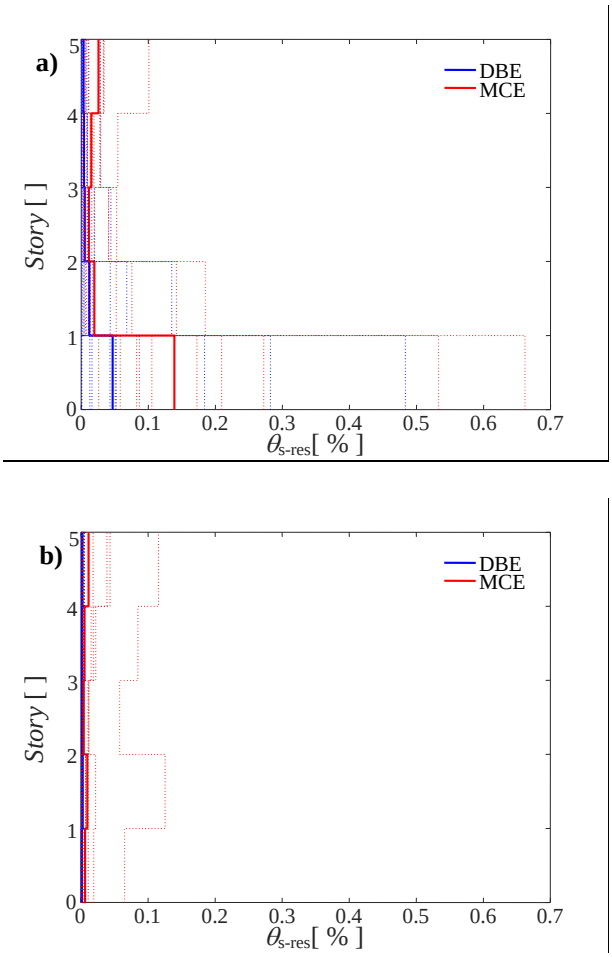

Figure 12. Residual interstory drifts from nonlinear dynamic analysis for the scaled ground motions for the DBE and MCE intensities for (a) SC-MRF (b) SC-MRF with column bases

5 CONCLUSIONS

The paper briefly summarizes some of the research outcomes of an extensive work on an innovative damage-free self-centering steel column base. The column base uses post-tensioned (PT) high strength steel bars to control rocking behavior and friction devices (FDs) to dissipate seismic energy.

The analytical formulation defined in order to describe the moment-rotation behaviors was presented together with the proposed design procedure for the calibration of the main design parameters. The design procedure aims at achieving the damage-free behavior, the self-centering capability and an adequate energy dissipation capacity of the column base.

Following this procedure, a column base was extracted from a prototype building, designed and built in order to experimentally evaluate the performance of the proposed column base under monotonic and cyclic quasi-static loads.

A three-dimensional non-linear finite element model of the column base was developed in ABAQUS in order to investigate the local behavior of the components, to validate the moment-rotation analytical equations and to demonstrate the efficiency of the design procedure.

The comparison between the experimental and the numerical results in ABAQUS shows a good agreement especially when local imperfections are introduced to the rocking interface. These imperfections slightly change the behavior of the column base and slightly influence the self-centering capabilities, however the damage-free behavior is affected. In fact, the tests demonstrate that the column base is damage-free for displacements up to the target design rotation and has the ability to limit the damage only to few easily replaceable components under much large rotations.

In addition, a simplified model for the column base was developed in OpenSees and allow to investigate the effects of the proposed column base on a case study building. The nonlinear dynamic analyses were performed by 10 ground motion records scaled to the Design Based Earthquake and the Maximum Credible Earthquake for the considered sites. The results of the analyses show that the rocking column base fully protects the 1st story columns from yielding and eliminate the 1st story residual story drift without any detrimental effect on peak story drifts.

The study demonstrates the high potential of the proposed innovative damage-free self-centering column base to be used for the definition of highly resilient steel structures.

REFERENCES

This research is supported by Marie Sklodowska-Curie Action Fellowships within the H2020 European Programme. Any opinions, findings, and conclusions or recommendations expressed in this paper are those of the authors and do not necessarily reflect the views of the European Commission.

REFERENCES

ABAQUS/Standard and ABAQUS/Explicit 2016. ABAQUS Theory Manual. *Dassault Systems*.

Borzouie, J., MacRae, G.A., Chase, J.G., Rodgers, G.W., Clifton, G.C., 2016. Experimental studies on cyclic performance of column base strong axis – aligned asymmetric friction connections. *Journal of Structural Engineering (ASCE)*, **142**(1): 04015078.

BS 5896, 2012. High tensile steel wire and strand for the prestressing of concrete. *British Standards Institution*.

Chancellor, N.B., Eatherton, M.R., Roke, D.A., Akbas, T., 2014. Self-centering seismic lateral force resisting systems: High-performance structures for the city of tomorrow. *Buildings*, **4**: 520-548.

Chi, H., Liu, J., 2012. Seismic behaviour of post-tensioned column base for steel self-centering moment resisting frame. *Journal of Constructional Steel Research*, **78**, 117–130.

Chou, C.-C., Chen, J.H., 2011. Analytical model validation and influence of column bases for seismic responses of steel post-tensioned self-centering MRF systems. *Engineering Structures*, **33**(9): 2628–2643.

Christopoulos, C., Filiatrault, A., 2006. Principles of passive supplemental damping and seismic isolation. *IUSS Press*, Pavia, Italy.

Dimopoulos, A.I., Karavasilis, T.L., Vasdravellis, G., Uy, B., 2013. Seismic design, modelling and assessment of self-centering steel frames using post-tensioned connections with web hourglass shape pins. *Bulletin of Earthquake Engineering*, **11**(5): 1797–1816.

Dimopoulos, A.I., Tzimas, A.S., Karavasilis, T.L., Vamvatsikos, D., 2016. Probabilistic economic seismic loss estimation in steel buildings using post-tensioned moment-resisting frames and viscous dampers. *Earthquake Engineering & Structural Dynamics*, **45**(11), 1725-1741.

Eurocode 3, 2005. Design of steel structures – Part 1.8: Design of Joints. *European Committee for Standardization*, Brussels, Belgium.

Eurocode 8, 2005. Design of structures for earthquake resistance. Part 1: General rules, seismic action and rules for buildings. *European Committee for Standardization*, Brussels, Belgium.

Federal Emergency Management Agency, 2000. FEMA 350: Recommended seismic design criteria for new steel moment frame buildings. *SAC Joint Venture*, Washington, DC.

Federal Emergency Management Agency, 2008. FEMA P695: Quantification of building seismic performance factors. ATC-63 Project. *Applied Technology Council*,

CA. USA.
Freddi, F., Tubaldi, E., Ragni, L., Dall'Asta, A. 2013. Probabilistic performance assessment of low-ductility reinforced concrete frame retrofitted with dissipative braces. *Earthquake Engineering & Structural Dynamics*, **42**(7): 993–1011.
Freddi, F., Dimopoulos, C.A., Karavasilis, T.L., 2017a. Rocking damage-free steel column base with friction devices: design procedure and numerical evaluation. *Earthquake Engineering & Structural Dynamics*, **46**(14): 2281–2300.
Freddi, F., Padgett, J.E., Dall'Asta, A. 2017b. Probabilistic Seismic Demand Modeling of Local Level Response Parameters of an RC Frame. *Bulletin of Earthquake Engineering*, **15**: 1-23.
Garlock, M., Sause, R., Ricles, J.M., 2007. Behavior and design of posttensioned steel frame systems. *Journal of Structural Engineering (ASCE)*, **133**(3): 389–399.
Gioiella, L., Tubaldi, E., Gara, F., Dezi, L., Dall'Asta A. 2018 Modal properties and seismic behaviour of buildings equipped with external dissipative pinned rocking braced frames. *Engineering Structures*; **172**: 807–819.
Grauvilardell, J.E., Lee, D., Hajjar, J.F., Dexter, R.J., 2006. Synthesis of design, testing and analysis research on steel column base plate connections in high-seismic zones, Report ST-04-02, *Dept. of Civil Engineering, Univ. of Minnesota*, USA.
Kamperidis, V.C., Karavasilis, T.L., Vasdravellis, G., 2018. Self-centering steel column base with metallic energy dissipation devices. *Journal of Constructional Steel Research*, **149**: 14–30.
Kanvinde, A.M., Grilli, D.A., Zareian, F., 2012. Rotational stiffness of exposed column base connections: experiments and analytical models. *Journal of Structural Engineering*, **138**(5): 549–560.
Latour, M., Rizzano, G., 2013a. Full strength design of column base connections accounting for random material variability. *Engineering Structures*, **48**: 458–471.
Latour, M., Rizzano, G., 2013b. A theoretical model for predicting the rotational capacity of steel base joints. *Engineering Structures*, **91**: 89–99.
Latour, M., Rizzano, G., Santiago, A., da Silva, L.S., 2019. Experimental response of a low-yielding, re-centering, rocking base plate joint with friction dampers. *Soil Dynamics and Earthquake Engineering*, **116**: 580-592.
Mackinven, H., MacRae, G.A., Pampanin, S., Clifton, G.C., Butterworth, J., 2007. Generation four steel moment frame joints. *Proceedings of the 8th Pacific Conference on Earthquake Engineering*, Singapore.
MacRae, G.A., Urmson, C.R., Walpole, W.R., Moss, P., Hyde, K., Clifton, C., 2009. Axial shortening of steel columns in buildings subjected to earthquakes. *Bulletin of the New Zealand Society for Earthquake Engineering*, **42**(4): 275–287.
Mahdavifar, V., Barbosa, A.R., Sinha, A., Muszynski, L., Gupta, R., Pryor, S.E., 2019. Hysteretic Response of Metal Connections on Hybrid Cross-Laminated Timber Panels. *Journal of Structural Engineering* (United States), **145**(1): 04018237.
McKenna, F., Fenves, G.L., Scott, M.H., 2006. OpenSees: Open system for earthquake engineering simulation, *PEER Center*, Berkeley, CA.
Rodas, P.T., Zareian, F., Kanvinde, M., 2016. Hysteretic model for exposed column-base connections, *Journal of Structural Engineering (ASCE)*, **142**(12): 04016137.
Tzimas, A.S., Dimopoulos, A.I., Karavasilis, T.L., 2015. EC8-based seismic design and assessment of self-centering post-tensioned steel frames with viscous dampers. *Journal of Constructional Steel Research*, **105**: 60–73.
Yamanishi, T., Kasai, K., Takamatsu, T., Tamai, H., 2012. Innovative column-base details capable of tuning rigidity and strength for low to medium-rise steel structures, *Proceedings of the 15th World Conference on Earthquake Engineering*, Lisbon, Portugal.
Wang, X.T., Xie, C.D., Lin, L.H., Li, J., 2019. Seismic behavior of self-centering concrete-filled square steel tubular (CFST) column Base. *Journal of Constructional Steel Research*, **156**: 75 – 85.
Zareian, F., Kanvinde, A., 2013. Effect of column-base flexibility on the seismic response and safety of steel moment-resisting frames, *Earthquake Spectra*, **29**(4): 1537–1559.